

# Learning Fair Representations via Rate-Distortion Maximization

Somnath Basu Roy Chowdhury    Snigdha Chaturvedi

{somnath, snigdha}@cs.unc.edu  
UNC Chapel Hill

## Abstract

Text representations learned by machine learning models often encode undesirable demographic information of the user. Predictive models based on these representations can rely on such information resulting in biased decisions. We present a novel debiasing technique **Fairness-aware Rate Maximization (FaRM)**, that removes demographic information by making representations of instances belonging to the same protected attribute class uncorrelated using the rate-distortion function. FaRM is able to debias representations with or without a target task at hand. FaRM can also be adapted to simultaneously remove information about multiple protected attributes. Empirical evaluations show that FaRM achieves state-of-the-art performance on several datasets, and learned representations leak significantly less protected attribute information against an attack by a non-linear probing network.<sup>1</sup>

## 1 Introduction

Democratization of machine learning has led to the deployment of statistical predictive models for critical applications like credit approval (Ghailan et al., 2016) and college application reviewing (Basu et al., 2019). For such applications, it is important to ensure that decisions made by the models are *fair* towards different demographic groups (Mehrabi et al., 2019). Fairness can be achieved by ensuring demographic information does not get encoded in representations used by these predictive models (Blodgett et al., 2016; Elazar and Goldberg, 2018; Elazar et al., 2021).

However, controlling demographic information encoded by a model’s representations is a challenging task for textual data. This is because natural language text is highly indicative of an author’s

<sup>1</sup>Work in progress.

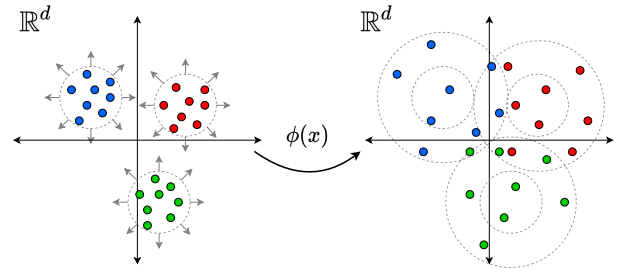


Figure 1: Illustration of unconstrained debiasing using FaRM. Data representations in different protected attribute class are shown in blue, red and green. Before debiasing representations from each class are similar to each other and information content in each subset is low. Debiasing using  $\phi(x)$  enforces the same class representations to be uncorrelated by increasing their information content.

demographic attributes even when it is not explicitly mentioned (Koppel et al., 2002; Burger et al., 2011; Nguyen et al., 2013; Verhoeven and Daelemans, 2014; Weren et al., 2014; Rangel et al., 2016; Verhoeven et al., 2016; Blodgett et al., 2016).

In this work, we focus on *debiasing* information about a protected demographic attribute from textual data representations. Prior works (Bolukbasi et al., 2016; Ravfogel et al., 2020) on debiasing involve projecting representations in a subspace that does not reveal demographic attribute information. These methods are only able to guard protected attributes against an attack by a linear function, while losing significant information present in the original representations (Ravfogel et al., 2020). Another line of work (Xie et al., 2017; Basu Roy Chowdhury et al., 2021) removes demographic information while retaining information about a target attribute  $y$  in an adversarial framework. However, adversarial methods are difficult to train and cannot perform debiasing without a target task at hand.

We present a novel debiasing technique **Fairness-aware Rate Maximization (FaRM)** that removes

demographic information by controlling the *rate-distortion* function of the learned representations. Intuitively, in order to remove information about a protected attribute from a set of representations, we want the representations of instances from the same protected attribute class to be uncorrelated to each other. We achieve this by maximizing the number of bits (rate-distortion) required to encode representations from the same protected attribute class. An illustration of the process is shown in Figure 1. The representations are shown as points in a two-dimensional feature space, color-coded according to their protected attribute class. FaRM learns a function  $\phi(x)$  such that representations of the same protected class become uncorrelated and similar to other representations, thereby making it difficult to extract the information about the protected attribute from the learned representations.

We perform rate-distortion maximization based debiasing in the following setups: (a) *unconstrained debiasing* - we remove information about a protected attribute  $g$  while retaining as much other information as possible, and (b) *constrained debiasing* - we retain information about a target attribute  $y$  while removing information pertaining to  $g$ . For unconstrained debiasing, we evaluate FaRM for removing gender information from word embeddings and demographic information from text representations that can then be used for a downstream NLP task (we show their utility for biography and sentiment classification in our experiments). Our empirical evaluations show that representations learned using FaRM in an unconstrained setup, leak significantly less protected attribute information compared to prior approaches against an attack by a non-linear probing network.

For constrained debiasing, FaRM achieves state-of-the-art debiasing performance on 3 datasets, and representations are able to guard protected attribute information significantly better than previous approaches. We also perform experiments to show that FaRM is able to remove multiple protected attributes simultaneously, while guarding against intersectional group biases (Subramanian et al., 2021). To summarize, our main contributions are:

- We present a novel framework **F**airness-aware **R**ate **M**aximization (FaRM) to perform debiasing in unconstrained and constrained setups, by controlling the rate-distortion function of textual data representations.
- Empirical evaluations show FaRM leaks signifi-

cantly less protected attribute information against a non-linear probing attack, outperforming prior approaches.

- We present two variations of FaRM for debiasing multiple protected attributes simultaneously, that are also effective against an attack for intersectional group biases.
- We perform various analysis experiments to understand the functioning of FaRM.

## 2 Related Work

Removing sensitive attributes from data representations for fair classification was initially introduced as an optimization task (Zemel et al., 2013). Subsequent works have used adversarial frameworks (Goodfellow et al., 2014) for this task (Zhang et al., 2018; Li et al., 2018; Xie et al., 2017; Elazar and Goldberg, 2018; Basu Roy Chowdhury et al., 2021). However, adversarial networks are hard to train (Elazar and Goldberg, 2018) and cannot function without a target task at hand.

Unconstrained debiasing frameworks focus on removing a protected attribute from representations, without relying on a target task. Bolukbasi et al. (2016) demonstrated that GloVe embeddings encode sensitive gender information and proposed an unconstrained debiasing framework for identifying the direction that represents gender and neutralizing vectors along that direction. Building on this approach, Ravfogel et al. (2020) proposed INLP, a robust framework to debias representations in an unconstrained manner by iteratively identifying protected attribute subspaces and projecting representations onto the corresponding nullspaces. Dev et al. (2020) demonstrated that the nullspace projection approach can be applied in a constrained setup as well. However, these approaches fail to guard protected information against an attack by a non-linear probing network.

In contrast to prior works, we present a novel debiasing framework based on the principle of rate-distortion maximization. Coding rate maximization was first introduced as an objective function by Ma et al. (2007) for image segmentation. This framework has also proved useful in explaining feature selection by neural networks (Macdonald et al., 2019). Recently, Yu et al. (2020) proposed maximal coding rate (MCR<sup>2</sup>) based on rate-distortion theory, a representation-level objective function that can serve as an alternative to conventional empirical risk minimization approaches. Our work

adopts a similar approach to MCR<sup>2</sup> but instead of learning representations for classification, we leverage rate maximization to remove protected information from representations.

### 3 Preliminaries

In this section, we introduce the fundamentals of rate-distortion theory that serve as building blocks of our proposed framework.

**Rate Distortion.** In lossy data compression, the compactness of a random distribution is measured by the minimal number of binary bits required to encode it, upto a precision  $\epsilon^2$ . A lossy coding scheme encodes a finite set of vectors  $Z = \{z_1, \dots, z_n\} \in \mathbb{R}^{n \times d}$  from a distribution  $P(Z)$ , such that the decoded vectors  $\{\hat{z}_i\}_{i=1}^n$  can be recovered upto a precision  $\mathbb{E}[\|z_i - \hat{z}_i\|^2] < \epsilon^2$ . The *rate-distortion* function  $R(Z, \epsilon)$  measures the minimal number of bits per vector required to encode the sequence  $Z$ .

Depending on the family of distribution  $P(Z)$ , we can choose a coding scheme that yields the optimal rate-distortion  $R(Z, \epsilon)$ . In case the vectors  $\{z_i\}_{i=1}^n$  are i.i.d. samples from a zero-mean multi-dimensional Gaussian distribution  $\mathcal{N}(0, \Sigma)$ , the optimal rate-distortion function is given as:

$$R(Z, \epsilon) = \frac{1}{2} \log_2 \det \left( I + \frac{d}{n\epsilon^2} ZZ^T \right) \quad (1)$$

where  $ZZ^T = \Sigma$  is the covariance matrix of the Gaussian distribution. In rate-distortion theory, we need  $nR(Z, \epsilon)$  bits to encode  $n$  vectors of  $Z$ . The optimal codebook depends on data dimension. Therefore, we need an additional  $dR(Z, \epsilon)$  bits to encode it. Finally, the total number of bits required to encode the sequence  $Z$  are:

$$\begin{aligned} \mathcal{L}(Z) &= (n + d)R(Z, \epsilon) \\ &= \left( \frac{n + d}{2} \right) \log_2 \det \left( I + \frac{d}{n\epsilon^2} ZZ^T \right) \end{aligned} \quad (2)$$

Ma et al. (2007) showed that  $\mathcal{L}(Z)$  provides a tight bound on the number of bits required to encode  $Z$  even in cases where the underlying distribution  $P(Z)$  is degenerate.

To summarize, a set of compact vectors (text representations) would require a low number of bits to encode, which would correspond to a low value of  $R(Z, \epsilon)$  and vice versa.

**Rate Distortion for a mixed distribution.** In general, the set of vectors  $Z$  can be from a mixture distribution (e.g. feature representations for multi-class data). The rate-distortion function can be

computed precisely if we split the data into multiple subsets:  $Z = Z^1 \cup Z^2 \dots \cup Z^k$ , based on their distribution. For each subset, we can accurately compute the  $R(Z^i, \epsilon)$  (Equation 1). To facilitate the computation, we define a membership matrix  $\Pi_j$  for each subset  $j$  as follows:

$$\Pi_j = \text{diag}(\pi_{1j}, \pi_{2j}, \dots, \pi_{nj}) \in \mathbb{R}^{n \times n} \quad (3)$$

where  $\pi_{ij} \in [0, 1]$  denotes the probability of vector  $z_i$  belonging to the  $j^{\text{th}}$  subset and  $n$  is the total number of vectors. The following conditions must be satisfied:  $\sum_j \pi_{ij} = 1$  and  $\sum_j \Pi_j = I_{n \times n}$ . The expected number of vectors in the  $j^{\text{th}}$  subset is  $\text{tr}(\Pi_j)$  and the corresponding covariance:  $\frac{1}{\text{tr}(\Pi_j)} Z \Pi_j Z^T$ . The overall rate-distortion function for the entire set  $Z$  is given as:

$$\begin{aligned} R^c(Z, \epsilon | \Pi) &= \\ &= \sum_{j=1}^k \frac{\text{tr}(\Pi_j)}{2n} \log_2 \det \left( I + \frac{d}{\text{tr}(\Pi_j)\epsilon^2} Z \Pi_j Z^T \right) \end{aligned} \quad (4)$$

In scenarios where a vector  $z_i$  can only be a member of a single class, we restrict  $\pi_{ij} = \{0, 1\}$  and covariance matrix for subset  $j$  is  $Z^j Z^{jT}$ .

## 4 Fairness-Aware Rate Maximization

In this section, we discuss using FaRM to learn fair representations in unconstrained and constrained debiasing setups.

### 4.1 Unconstrained Debiasing using FaRM

In this setup, we aim to remove information about a protected attribute  $\mathbf{g}$  from data representations  $X$  while retaining the remaining information. To achieve this, the debiased representations  $Z$  should have the following properties:

(a) *Intraclass Incoherence*: Representations belonging to the same protected attribute class should be highly uncorrelated. This would make it difficult for a probing network to extract any information about  $\mathbf{g}$  from the representations.

(b) *Maximal Informativeness*: Representations should be maximally informative about remaining information. The rank of the learned representations should be large, increasing the number of bits required to encode all representations.

Assuming there are  $k$  protected attribute classes, we can write  $Z = Z^1 \cup \dots \cup Z^k$ . To achieve (a), we need to ensure that the representations in a subset  $Z^j$  belonging to the same protected class do

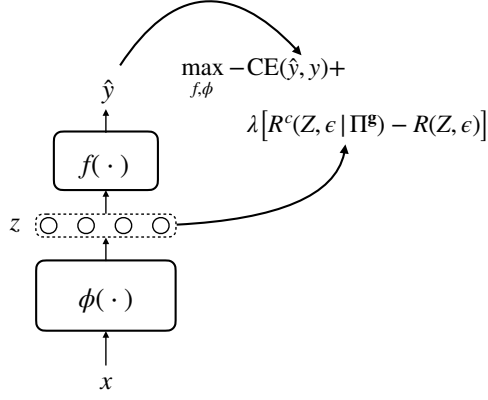


Figure 2: Constrained debiasing setup using FaRM. Representation  $z$  retrieved from the feature map  $\phi$  is used to predict the target label and control the rate-distortion objective function.

not lie in a low-dimensional subspace and the rate-distortion function  $R^c(Z, \epsilon | \Pi^g)$  is *large*. For (b), we want the representations  $Z$  to retain maximal possible information from the input  $X$ . If the *information content* in  $Z$  is large then the number of bits required to encode it – rate-distortion  $R(Z, \epsilon)$  should also be *large*. FaRM achieves (a) and (b) simultaneously by maximizing the following objective function:

$$J_u(Z, \Pi^g) = R(Z, \epsilon) + R^c(Z, \epsilon | \Pi^g) \quad (5)$$

where the partition function  $\Pi^g$ , is constructed using the protected attribute  $g$  (see Equation 3).

We use a deep neural-network  $\phi(\cdot)$  as our feature map to obtain debiased representations  $z = \phi(x)$ . The objective function  $J_u$  is used to learn the parameters of the feature map  $\phi$ .  $J_u$  is sensitive to the scale of the representations, therefore we normalize the Frobenius norm of the representations to ensure individual input samples have an equal impact on the loss. We use layer normalization (Ba et al., 2016) that ensures all representations have the same magnitude and lie on a sphere  $z_i \in \mathbb{S}^{d-1}(r)$  of radius  $r$ . We obtain the parameters of  $\phi$  using the following objective function:

$$\hat{\phi} = \arg \max_{\phi} [R(Z, \epsilon) + R^c(Z, \epsilon | \Pi^g)] \quad (6)$$

An illustration of the debiasing process in the unconstrained setup is shown in Figure 1.

## 4.2 Constrained Debiasing using FaRM

In this setup, we aim to remove information about a protected attribute  $g$  from data representations  $X$

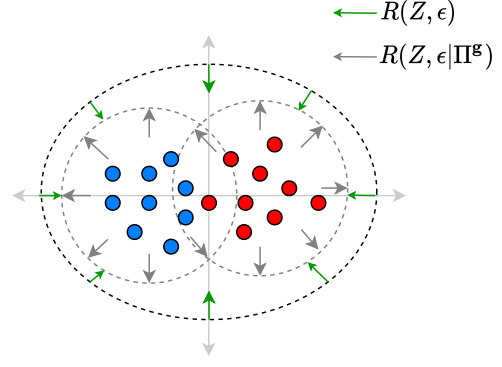


Figure 3: Visualization for regularization loss in  $J_c$  for constrained debiasing. The **red** and **blue** circles represent 2D representations from two different protected class. The **gray** arrows are induced by  $R^c(Z, \epsilon | \Pi^g)$  term and the **green** ones are induced by  $R(Z, \epsilon)$  term in the objective function.

while retaining information about a specific target attribute  $y$ . After debiasing, the learned classifier should perform well on the target task of predicting  $y$  without relying on information from the protected attribute  $g$ . The learned representations should have the following properties:

- (a) *Target-Class Informativeness*: Representations should be maximally informative about the target task attribute  $y$ .
- (b) *Interclass Coherence*: Representations from different protected attribute classes should be *similar* to each other. This would make it difficult to extract information about  $g$  from  $Z$ .

Our constrained debiasing setup is shown in Figure 2, where representations are retrieved from a feature map  $\phi(\cdot)$  followed by a target task classifier  $f(\cdot)$ . In this setup, we achieve (a) by training  $f$  to predict the target class  $\hat{y} = f(z)$  and minimize the cross-entropy loss  $\text{CE}(\hat{y}, y)$ , where  $y$  is the ground-truth target label. For (b), we need to ensure that representations from different protected class are similar and overlap in the representation space. This is achieved by *maximizing* the rate  $R^c(Z, \epsilon | \Pi^g)$  to make samples in the same protected class dissimilar while ensuring the *compactness* of the entire space by minimizing  $R(Z, \epsilon)$ . A visualization for the process is illustrated in Figure 3. The **blue** and **red** circles correspond to representations from two different protected classes. The **gray** arrows are induced by the term  $R^c(Z, \epsilon | \Pi^g)$  that encourages the representations to be dissimilar to samples in the same protected class. The **green** arrows induced by  $R(Z, \epsilon)$  tries to make the rep-

resentation space more compact. To achieve (b), FaRM adds a rate-distortion based regularization constraint to the target classification loss. Overall, FaRM achieves (a) and (b) simultaneously by maximizing the following objective function:

$$J_c(Z, Y, \Pi^g) = -\text{CE}(\hat{y}, y) + \lambda [R^c(Z, \epsilon | \Pi^g) - R(Z, \epsilon)] \quad (7)$$

where  $\hat{y}$  is the target prediction label,  $y$  is the ground-truth target label and  $\lambda$  is a hyperparameter.<sup>2</sup>

## 5 Experimental Setup

In this section, we discuss the datasets, experimental setup, and metrics used for evaluating FaRM.

### 5.1 Datasets

We evaluate FaRM for constrained and unconstrained debiasing using several datasets described below. Among these, DIAL and Biographies datasets are used for evaluating both the constrained and unconstrained debiasing. PAN16 and GloVe embeddings are used only for constrained and unconstrained debiasing respectively.

(a) **DIAL** (Blodgett et al., 2016) is a Twitter-based sentiment classification dataset. Each tweet is associated with a sentiment label (treated as the *target attribute* in constrained evaluation) and “race” information (*protected attribute*) of the author. The sentiment labels are “happy” or “sad” and race categories are “African-American English” (AAE) or “Standard American English” (SAE). We use the same train-test split as Elazar and Goldberg (2018).

(b) **Biography classification** dataset (De-Arteaga et al., 2019) contains biographies that are associated with a profession (*target attribute*) and gender label (*protected attribute*). The profession can be categorized into 28 different classes and gender is a binary attribute. The dataset has been retrieved and processed from the open-sourced project.<sup>3</sup> We use the same train-dev-test split of 65:10:25 as the authors (De-Arteaga et al., 2019). For certain professions like “professor” or “nurse”, gender label is highly correlated with the target task. This makes

<sup>2</sup>Note, we cannot use the same regularization term (Equation 7) for unconstrained debiasing as minimizing  $R(Z, \epsilon)$  without the additional supervision of target loss  $\text{CE}(\hat{y}, y)$  will allow representations to converge to a compact space, thereby losing most information. We verify this phenomenon in an ablation experiment (more details in Appendix A.1).

<sup>3</sup><https://github.com/Microsoft/biosbias>

this dataset an interesting case study to investigate whether it is possible to infer profession without gender information.

(c) **PAN16** (Rangel et al., 2016) is also a Tweet-classification dataset where each Tweet is annotated with the author’s age and gender information both of which are protected attributes. The target task is mention detection. We use the same train-test split as Elazar and Goldberg (2018).

(d) **GloVe embeddings**: We follow the setup of Ravfogel et al. (2020) to debias most common 150,000 Glove word embeddings (Zhao et al., 2018). For training we use 7500 most male-biased, female-biased and neutral words (determined by the magnitude of each word vector’s projection onto the  $\vec{he} - \vec{she}$  direction). The data is randomly divided into a 70:30 split training and test set.

### 5.2 Implementation details

We use a mutli-layer neural network with ReLU non-linearity as our feature map  $\phi$  in the unconstrained setup. This setup is optimized using stochastic gradient descent with a learning rate of 0.001 and momentum of 0.9. For constrained debiasing, we used BERT<sub>base</sub> as  $\phi$ , and a 2-layer neural network as  $f$ . Constrained setup is optimized using AdamW (Loshchilov and Hutter, 2019) optimizer with a learning rate of  $2 \times 10^{-5}$ . We set  $\lambda = 0.01$  for all experiments. Hyperparameters were tuned on the development set of the respective datasets. Our models were trained on a single Nvidia Quadro RTX 5000 GPU.

### 5.3 Probing Metrics

Following (Elazar and Goldberg, 2018; Ravfogel et al., 2020; Basu Roy Chowdhury et al., 2021), we evaluate the quality of our debiasing by probing the learned representations. After debiasing, we retrieve the representations from the feature map  $\phi(x)$  and train separate probing networks for the protected attribute  $\mathbf{g}$  and target attribute  $\mathbf{y}$ . In our experiments, we probe all representations using a non-linear classifier.<sup>4</sup> We report the Accuracy and Minimum Description Length (MDL) (Voita and Titov, 2020) for predicting  $\mathbf{g}$  and  $\mathbf{y}$ . A large MDL signifies that more effort is needed by a probing network to achieve a certain performance. Hence, we expect the debiased representations to have *large* MDL for protected attribute  $\mathbf{g}$  and a *small* MDL

<sup>4</sup>We use a MLP Classifier from scikit-learn library (Pedregosa et al., 2011).

for predicting target attribute  $\mathbf{y}$ . Also, we expect a *high* accuracy for  $\mathbf{y}$  and *low* accuracy for  $\mathbf{g}$ .

## 5.4 Group Fairness Metrics

**TPR-GAP.** De-Arteaga et al. (2019) introduced this measure to evaluate the fairness of a classifier. TPR-GAP is based on the notion of *equalized odds*, which requires the true positive rate (TPR) between two protected groups to be similar. For a classification task with target attribute  $\mathbf{y}$  and a binary protected attribute  $\mathbf{g}$ , TPR-GAP for a target attribute label  $y$  is defined as:

$$\text{TPR}_{\mathbf{g},y} = p(\hat{\mathbf{y}} = y | \mathbf{g} = g, \mathbf{y} = y) \quad (8)$$

$$\text{Gap}_{\mathbf{g},y} = \text{TPR}_{g,y} - \text{TPR}_{\bar{g},y} \quad (9)$$

where  $\mathbf{y}$  is the target attribute,  $\mathbf{g}$  is a binary protected attribute with possible labels  $-g, \bar{g}$ , and  $\hat{\mathbf{y}}$  denote the predicted target attribute.

Following (Romanov et al., 2019), we obtain a single bias score by computing the root mean square of  $\text{Gap}_{\mathbf{g},y}$  for all target labels  $y$ .  $\text{Gap}_{\mathbf{g}}^{\text{RMS}}$  score is defined as:

$$\text{Gap}_{\mathbf{g}}^{\text{RMS}} = \sqrt{\frac{1}{|\mathcal{Y}|} \sum_{y \in \mathcal{Y}} (\text{Gap}_{\mathbf{g},y})^2} \quad (10)$$

where  $\mathcal{Y}$  is the set of target attribute labels.

**Demographic Parity (DP).** DP measures the difference in prediction w.r.t to the protected attribute  $\mathbf{g}$ . Formally, it is defined as:

$$\text{DP} = \sum_{y \in \mathcal{Y}} |p(\hat{\mathbf{y}} = y | \mathbf{g} = g) - p(\hat{\mathbf{y}} = y | \mathbf{g} = \bar{g})| \quad (11)$$

where  $g, \bar{g}$  are possible values of the binary protected attribute  $\mathbf{g}$  and  $\mathcal{Y}$  is the set of possible target attribute labels. We compute the prediction difference across all  $\mathcal{Y}$ .

Zhao and Gordon (2019) demonstrated an inherent tradeoff between the utility and fairness of representations. TPR-GAP described above is not a good indicator of fairness if  $\mathbf{y}$  and  $\mathbf{g}$  are correlated, as debiasing would lead to a drop in target task performance as well. While learning fair representations, we actually optimize for Demographic Parity. We report our performance using both metrics for completeness. However, in few setups we observe conflicting results using these metrics.

Method	Accuracy ( $\downarrow$ )	MDL ( $\uparrow$ )	Rank ( $\uparrow$ )
GloVe	100.0	0.1	300
INLP	86.3	8.6	210
FaRM	<b>53.9</b>	<b>24.6</b>	<b>247</b>

Table 1: Debiasing performance on Glove word embeddings. We report the Accuracy, MDL of gender attribute and embedding matrix rank. FaRM significantly outperforms INLP (Ravfogel et al., 2020) in guarding gender information.

## 6 Results: Unconstrained Debiasing

We evaluate FaRM for unconstrained debiasing in different 3 setups following Ravfogel et al. (2020): word embedding debiasing, and debiasing text representations for fair biographies classification and fair sentiment classification. For the classification tasks, we retrieve text representations from a pre-trained encoder, debias them using FaRM (without taking target task into account) and evaluate the quality of debiased representations by probing for target and protected tasks. All tables reporting the results mention the expected trend of a metric using  $\uparrow$  – higher or  $\downarrow$  – lower.

### 6.1 Word Embedding Debiasing

We revisit the problem of debiasing gender information from word embeddings introduced by Bolukbasi et al. (2016).

**Setup.** We debias gender information from GloVe embeddings using a 4-layer neural network with ReLU non-linearity as the feature map  $\phi(x)$ .<sup>5</sup>

**Results.** Table 1 presents the result of debiasing word embeddings. We observe that when compared with INLP, FaRM reduces the accuracy of the network by an absolute margin of 32.4% and achieves a steep increase in MDL. FaRM is able to guard protected attribute against an attack by a non-linear probing network (near random accuracy). Also, increase in rank of the resultant embedding matrix indicates that FaRM is able to retain more information in the representations, in general, compared to INLP.

**Visualization.** We visualize the t-SNE (Van der Maaten and Hinton, 2008) projections of Glove embeddings before and after debiasing in Figures 4a and 4b respectively. Female and male-biased word vectors are represented by **red** and **blue** dots respectively. The figures clearly demonstrate that the

<sup>5</sup>We discuss the choice of the feature map  $\phi$  in Section 8.

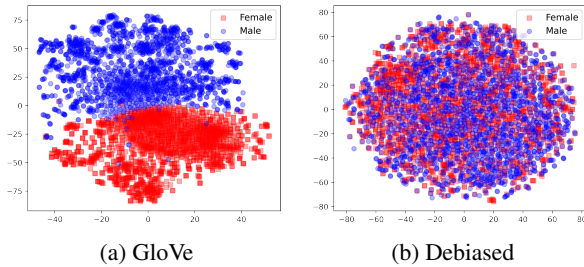


Figure 4: t-SNE projection of GloVe embeddings before (left) and after debiasing using FaRM (right). Initial female-biased vectors are shown in **red** and male-biased ones in **blue**.

gendered vectors are not separable after debiasing (Figure 4b). In order to quantify the improvement, we perform  $k$ -means clustering with  $K = 2$  (one for each gender label). We compute the V-measure (Rosenberg and Hirschberg, 2007), which is a measure to assess the degree of overlap between the clusters. V-measure in the original space drops from 99.9% to 0.006% using FaRM (compared to 0.31% using INLP). This indicates that debiased representations from FaRM are more difficult to disentangle. We further analyze the quality of the debiased word embeddings in Section 8.

## 6.2 Biography Classification

Next, we evaluate FaRM by debiasing text representations in an unconstrained setup and using the representation for fair biography classification.

**Setup.** We obtain the text representations using two methods: FastText (Joulin et al., 2017) and BERT (Devlin et al., 2019). For FastText, we sum the individual token representations in each biography. For BERT, by retrieving the final layer hidden representation of [CLS] token from a pre-trained BERT<sub>base</sub> model. We choose the feature map  $\phi(x)$  as 4-layer neural network with ReLU non-linearity.

**Results.** Table 2 presents the unconstrained debiasing results of FaRM on this dataset. ‘Original’ in the table refers to the pre-trained embeddings from BERT<sub>base</sub> or FastText. We observe that FaRM significantly outperforms INLP in fairness metrics – DP (improvement of 92% for FastText and 91% for BERT) and  $\text{Gap}_g^{\text{RMS}}$  (improvement of 93% for FastText and 18% for BERT). We observe that FaRM achieves near random gender classification performance (majority baseline=53.9%) against a non-linear probing attack. FaRM improves upon INLP’s gender prediction performance by an abso-

Metric	Method	FastText	BERT
Profession Acc. ( $\uparrow$ )	Original	79.9	80.9
	INLP	<b>76.3</b>	<b>77.8</b>
	FaRM	54.8	55.8
Gender Acc. ( $\downarrow$ )	Original	98.9	99.6
	INLP	67.4	94.9
	FaRM	<b>57.6</b>	<b>55.6</b>
DP ( $\downarrow$ )	Original	1.65	1.68
	INLP	1.51	1.50
	FaRM	<b>0.12</b>	<b>0.14</b>
$\text{Gap}_g^{\text{RMS}}$ ( $\downarrow$ )	Original	0.185	0.171
	INLP	0.089	0.096
	FaRM	<b>0.006</b>	<b>0.079</b>

Table 2: Evaluation results of FaRM on biographies dataset. Compared to INLP (Ravfogel et al., 2020), representations from FaRM leak significantly less gender information and achieve the best fairness scores. ‘Original’ refers to the pre-trained embeddings from BERT<sub>base</sub> or FastText.

lute margin of 9.8% and 39.4% for FastText and BERT respectively. However, we observe a substantial drop in the accuracy for identifying profession using the debiased embeddings. This is possibly because in this dataset, gender is highly correlated with profession and removing gender information makes it difficult to identify profession. In the unconstrained setup, we remove the information about the protected attribute from the representations without taking into account the target task. As a result target task performance suffers with more debiasing.<sup>6</sup> This calls for constrained debiasing for such datasets. In Section 7, we show that FaRM is able to retain target performance while debiasing for this dataset in the constrained setup.

## 6.3 Controlled Sentiment Classification

Lastly, for the DIAL dataset, we perform unconstrained debiasing in a controlled setting.

**Setup.** Following the setup of Barrett et al. (2019); Ravfogel et al. (2020), we control the proportion of protected attributes within a target-task class. For example, if target class split=80% that means ‘happy’ sentiment (target) class contains 80% AAE / 20% SAE, while the ‘sad’ class contains 20% AAE / 80% SAE (AAE and SAE are protected class labels mentioned in Section 5.1). We train

<sup>6</sup>In our experiments, we found profession accuracy to be high with a shallow feature map or training for lesser epochs, but the gender leakage was significant in these scenarios.

Metric	Method	Split			
		50%	60%	70%	80%
Sentiment Acc. ( $\uparrow$ )	Original	75.5	75.5	74.4	71.9
	INLP	<b>75.1</b>	73.1	<b>69.2</b>	<b>64.5</b>
	FaRM	74.8	<b>73.2</b>	67.3	63.5
Race Acc. ( $\downarrow$ )	Original	87.7	87.8	87.3	87.4
	INLP	69.5	82.2	80.3	69.9
	FaRM	<b>54.2</b>	<b>69.9</b>	<b>69.0</b>	<b>52.1</b>
DP ( $\downarrow$ )	Original	0.26	0.44	0.63	0.81
	INLP	0.16	0.33	0.30	0.28
	FaRM	<b>0.09</b>	<b>0.10</b>	<b>0.17</b>	<b>0.22</b>
Gap <sub>g</sub> <sup>RMS</sup> ( $\downarrow$ )	Original	0.15	0.24	0.33	0.41
	INLP	0.12	0.18	0.16	0.16
	FaRM	<b>0.09</b>	<b>0.10</b>	<b>0.12</b>	<b>0.14</b>

Table 3: We report the Sentiment Accuracy, Gender Accuracy, Gap<sub>g</sub><sup>RMS</sup> and Demographic parity of the original classifier, INLP (Ravfogel et al., 2020) and FaRM on DIAL dataset. We observe that FaRM achieves the best fairness scores in all setups, while maintaining similar performance on sentiment classification task. ‘Original’ refers to text embeddings from DeepMoji encoder.

DeepMoji (Felbo et al., 2017) followed by a 1-layer MLP for sentiment classification. We retrieve representations from the DeepMoji encoder and debias them using FaRM. For debiasing, we choose the feature map  $\phi(x)$  to be a 7-layer neural network with ReLU non-linearity. After debiasing, we train a non-linear MLP to investigate the quality of debiasing. We evaluate the debiasing performance of FaRM in various stages of label imbalance.

**Results.** The results of this experiment are reported in Table 3. We observe that FaRM is able to achieve the best fairness scores achieving an improvement in Gap<sub>g</sub><sup>RMS</sup> ( $\geq 12.5\%$ ) and DP ( $\geq 21\%$ ) across all setups. Considering accuracy of identifying the protected attribute – race, we can see that FaRM significantly reduces the leakage of race information by an absolute margin of 11%-17% across different target class splits. FaRM also achieves similar performance to INLP in sentiment classification. We observe that the fairness score for FaRM deteriorates with increasing correlation between protected attribute and target attribute. In cases where the target and the protected attributes are highly correlated (split=70% and 80%), we observe a low sentiment classification accuracy (for both INLP and FaRM) compared to the original classifier. This is similar to the observation made

for the Biographies classification dataset and shows that it is difficult to debias information about protected attribute while retaining overall information about the target task when the protected attribute is highly correlated with the target attribute. In the constrained setup, FaRM is able to retain target performance while debiasing for this dataset (Section 7).

## 7 Results: Constrained Debiasing

In this section, we present the evaluation results of constrained debiasing using FaRM. For all experiments, we use a BERT<sub>base</sub> model as our text encoder  $\phi$  and a 2-layer neural network with ReLU non-linearity as  $f$  (Figure 2).

### 7.1 Single Attribute Debiasing

In this setup, we focus on debiasing a single protected attribute  $g$  while retaining information about the target attribute  $y$ .

**Setup.** We conduct experiments on 3 datasets: DIAL (Blodgett et al., 2016), PAN16 (Rangel et al., 2016) and Biographies (De-Arteaga et al., 2019). We experiment with different target and protected attribute configurations in DIAL ( $y$ : Sentiment/Mention,  $g$ : Race) and PAN16 ( $y$ : Mention,  $g$ : Gender/Age). For Biographies, we use the same setup as described in Section 6.2. For the protected attribute  $g$ , we report  $\Delta F1$  – difference between F1-score and the majority baseline. For fair classification, we want  $\Delta F1$  to be *small* and MDL to be *large* for the protected attribute  $g$ . For target attribute  $y$ , we want F1 score to be *large* and MDL to be *small*. We also report fairness metrics: Gap<sub>g</sub><sup>RMS</sup> and Demographic Parity (DP) of the learned classifier. We compare FaRM with state-of-the-art AdS model (Basu Roy Chowdhury et al., 2021) and pre-trained BERT<sub>base</sub> representations.

**Results.** Table 4 presents the results of this experiment. We observe that FaRM achieves the best DP score in all setups. FaRM also beats AdS in Gap<sub>g</sub><sup>RMS</sup> for all settings except PAN16 (Age/Mention). In PAN16, FaRM achieves comparable performance to AdS in terms of MDL of the protected attribute  $g$ . FaRM achieves perfect fairness in terms of probing accuracy  $\Delta F1 = 0$ , and FaRM’s classifier learned is more fair in terms of DP compared to AdS. FaRM also achieves the best MDL score for the target attribute  $y$  on all datasets except Biographies (where the accuracy is the same as AdS). This shows that FaRM is able



Method	DIAL											
	Sentiment (y)		Race (g)		Fairness		Mention (y)		Race (g)		Fairness	
	F1↑	MDL↓	ΔF1↓	MDL↑	DP↓	Gap <sub>g</sub> <sup>RMS</sup> ↓	F1↑	MDL↓	ΔF1↓	MDL↑	DP↓	Gap <sub>g</sub> <sup>RMS</sup> ↓
BERT <sub>base</sub>	63.9	300.7	10.9	242.6	-	-	66.1	290.1	24.6	258.8	-	-
AdS	72.9	56.9	5.2	290.6	0.43	0.21	<b>81.1</b>	7.6	21.7	270.3	<u>0.06</u>	<u>0.03</u>
FaRM	<b>73.2</b>	<b>17.9</b>	<b>0.2</b>	<b>296.5</b>	<b>0.26</b>	<b>0.14</b>	78.8	<b>3.1</b>	<b>0.3</b>	<b>324.8</b>	<u>0.06</u>	<u>0.03</u>

Method	PAN16											
	Mention (y)		Gender (g)		Fairness		Mention (y)		Age (g)		Fairness	
	F1↑	MDL↓	ΔF1↓	MDL↑	DP↓	Gap <sub>g</sub> <sup>RMS</sup> ↓	F1↑	MDL↓	ΔF1↓	MDL↑	DP↓	Gap <sub>g</sub> <sup>RMS</sup> ↓
BERT <sub>base</sub>	72.3	259.7	7.4	300.5	-	-	72.8	262.6	6.1	302.0	-	-
AdS	<b>89.7</b>	7.6	4.9	<b>313.9</b>	0.04	0.007	<b>89.2</b>	6.0	1.1	<b>315.1</b>	0.04	<b>0.004</b>
FaRM	88.7	<b>1.7</b>	<b>0.0</b>	312.4	<b>0.04</b>	<b>0.007</b>	88.6	<b>0.8</b>	<b>0.0</b>	312.6	<b>0.03</b>	0.008

Method	BIOGRAPHIES							
	Profession (y)		Gender (g)		Fairness			
	F1↑	MDL↓	ΔF1↓	MDL↑	DP↓	Gap <sub>g</sub> <sup>RMS</sup> ↓		
BERT <sub>base</sub>	74.3	499.9	45.2	27.6	-	-		
AdS	99.9	<b>3.3</b>	<b>3.1</b>	449.5	0.45	0.003		
FaRM	<b>99.9</b>	7.6	7.4	<b>460.3</b>	<b>0.42</b>	<b>0.002</b>		

Table 4: Evaluation results for FaRM in constrained settings on DIAL, PAN16 and Biographies dataset. ΔF1 for the protected attribute g refers to F1-score difference with the majority baseline. FaRM outperforms AdS (Basu Roy Chowdhury et al., 2021) in Demographic Parity metric in all setups, while achieving comparable target task performance.

SETUP	PAN16											
	Mention (y)		Age (g <sub>1</sub> )		Fairness (g <sub>1</sub> )		Gender (g <sub>2</sub> )		Fairness (g <sub>2</sub> )		Inter. Groups (g <sub>1</sub> , g <sub>2</sub> )	
	F1↑	MDL↓	ΔF1↓	MDL↑	DP↓	Gap <sub>g</sub> <sup>RMS</sup> ↓	ΔF1↓	MDL↑	DP↓	Gap <sub>g</sub> <sup>RMS</sup> ↓	ΔF1↓	MDL↑
BERT <sub>base</sub> (fine-tuned)	88.6	6.8	14.9	196.4	0.06	0.009	69.3	192.0	0.04	0.014	20.7	117.2
AdS	<b>88.6</b>	<b>5.5</b>	2.2	231.5	0.05	0.006	1.6	230.9	0.04	0.017	9.1	118.5
FaRM (N-partition)	87.0	13.4	0.0	234.3	<b>0.03</b>	<b>0.003</b>	<u>0.0</u>	<u>234.2</u>	0.06	0.025	0.7	<b>468.0</b>
FaRM (1-partition)	86.4	15.6	<b>0.0</b>	<b>234.6</b>	0.05	0.006	<u>0.0</u>	<u>234.2</u>	<b>0.02</b>	<b>0.009</b>	<b>0.0</b>	467.7

Table 5: Evaluation results for debiasing multiple protected attributes using FaRM. Both configurations of FaRM significantly outperform the baseline AdS (Basu Roy Chowdhury et al., 2021) in removing protected attribute information, while guarding against intersectional group biases.

to robustly remove sensitive information about protected attribute information while achieving good target task performance.

## 7.2 Multiple Attribute Debiasing

In this setup, we focus on debiasing multiple protected attributes  $g_i$ 's simultaneously, while retaining information about target attribute  $y$ . We evaluate FaRM on PAN16 dataset with  $y$  – Mention,  $g_1$  – Gender, and  $g_2$  – Age. For protected attributes, we report the ΔF1 – the performance above majority baseline, MDL, Demographic Parity and Gap<sub>g</sub><sup>RMS</sup> scores. Subramanian et al. (2021) showed that debiasing a categorical attribute can still reveal information about intersectional groups (e.g. if age (young/old) and gender (male/female) are two categorical protected attributes, then (age=old, gender=male) is an intersectional group). To evaluate this leakage in our framework, we probe the learnt

representations for intersectional groups and report the corresponding ΔF1/MDL scores. We report the F1-score and MDL obtained by a probing network for target attributes.

**Approach.** We present two variations of FaRM in order to remove multiple attributes simultaneously in a constrained setup. Assuming there are  $N$  protected attributes ( $N > 1$ ), details of the variations are discussed below:

(a) *N-partition functions*: In the first variation, we obtain distinct partition function  $\Pi^{g_i}$  for each protected attribute  $g_i$ . We modify Equation 7 to obtain the following objective function:

$$J_c(Z, Y, \Pi^{g_1}, \dots, \Pi^{g_N}) = -\text{CE}(\hat{y}, y) + \lambda \sum_{i=1}^N [R(Z, \epsilon | \Pi^{g_i}) - R(Z, \epsilon)] \quad (12)$$

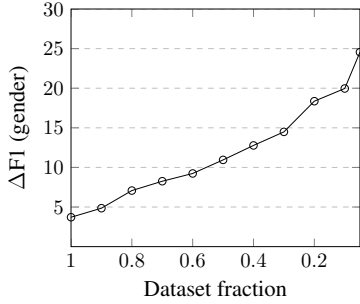


Figure 5:  $\Delta$ F1-score for gender prediction (leakage) in debiased word embeddings obtained from FaRM (unconstrained setup) with varying dataset fraction.  $\Delta$ F1-score is large when the size of dataset is small.

(b) *1-partition function*: Unlike the previous setup, we can consider each protected attribute  $\mathbf{g}_j$  as an independent variable and combine them to form a single protected attribute  $\mathcal{G}$ . For an input instance  $x_i$ , we can represent the  $j^{\text{th}}$  protected attribute as a one-hot vector  $\mathbf{g}_{ij} \in \mathbb{R}^{|\mathbf{g}_j|}$  (where  $|\mathbf{g}_j|$  is the dimension of protected attribute  $\mathbf{g}_j$ ). Then the combined vector  $\mathcal{G}^j \in \mathbb{R}^{(|\mathbf{g}_1|+\dots+|\mathbf{g}_N|)}$  can be obtained by concatenating individual vectors  $\mathbf{g}_{ij}$ . Since  $\mathcal{G}^j$  is a concatenation of multiple vectors, its norm can become large and so we normalize  $\mathcal{G}^j$  such that all of its elements sum to 1. Therefore each element of  $\mathcal{G}^j$  is either 0 or  $\frac{1}{N}$ . We use  $\mathcal{G}$  to construct the partition function  $\Pi^{\mathcal{G}}$ , which captures information about  $N$  attributes simultaneously. Each component of  $\Pi^{\mathcal{G}}$  satisfy:  $\sum_{j=1}^N \Pi_j^{\mathcal{G}} = I_{n \times n}$  and  $\pi_{ij} \in \{0, \frac{1}{N}\}$ . The resultant objective function takes the same form as in Equation 7 with the modified partition function  $J_c(Z, Y, \Pi^{\mathcal{G}})$ .

**Results.** We present the results of debiasing multiple attributes in Table 5. We observe that FaRM improves upon AdS’  $\Delta$ F1-score of age and gender with  $N$ -partition and 1-partition setups performing equally well. The performance on target task is comparable with AdS, although there is a slight rise in MDL. It is important to note that even though AdS’ performs decently well in preventing leakage about  $\mathbf{g}_1$  and  $\mathbf{g}_2$ , it still leaks a significant amount of information about the intersectional groups. In both of its configurations, FaRM is able to prevent leakage of intersectional biases while considering the protected attributes independently. This shows that robustly removing information about multiple attributes helps in preventing leakage about intersectional groups as well.

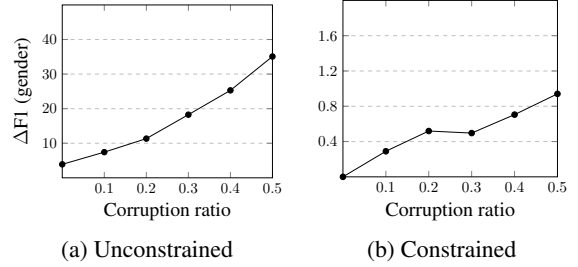


Figure 6: Performance of FaRM with varying fraction of corrupted training set labels in (a) unconstrained and (b) constrained debiasing setups.

## 8 Model Analysis

In this section, we present several analysis experiments to evaluate the functioning of FaRM.

**Sample Efficiency.** We investigate the sensitivity to the size of the training set of FaRM by systematically subsampling from the original dataset. In unconstrained setup, we experiment with word embedding debiasing and vary the size of the training set (shown in Figure 5). The  $\Delta$ F1-score on the  $y$ -axis is obtained by probing word embeddings for the gender label using a MLP classifier. We observe a gradual decline in performance (increase in  $\Delta$ F1) as the dataset size decreases. The drop in debiasing performance is within  $<10\%$  of the original performance even with 50% of the data. Even in extreme low data regime (5% data  $\sim$  400 samples), FaRM is able to protect gender information (gender prediction accuracy – 74.7%) better than baseline INLP (gender prediction accuracy – 86.3%) with access to full data (Table 1). This shows that FaRM is capable of removing protected attribute information with access to very few training samples.

**Robustness to label corruption.** Next, we evaluate the robustness of FaRM when the protected attribute labels are corrupted. We randomly subsample instances from the dataset and modify the protected attribute label. In Figure 6a, we report the gender leakage ( $\Delta$ F1 score) from the debiased word embeddings with varying fraction of the training set labels being corrupted. We observe that FaRM’s performance degrades with an increase in label corruption. This is expected and at high corruption ratios most of the protected attribute labels are wrong, leading to a poor performance.

In the constrained setup shown in Figure 6b, we observe that FaRM is able to debias information about a protected attribute even with a high protected label corruption ratio. We believe this en-

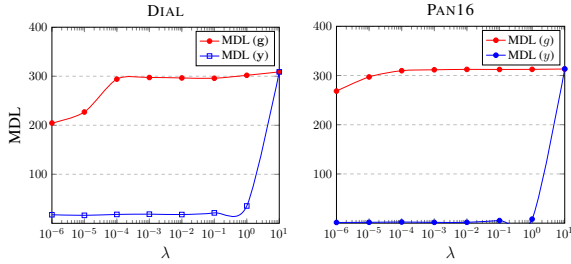


Figure 7: MDL of target ( $y$ ) and protected ( $g$ ) attributes with different  $\lambda$  in the constrained setup for DIAL and PAN16 datasets.

hanced performance (compared to unconstrained setup) is due to the fact that additional supervision is available in the form of target loss. The target loss can guide the model to learn robust representations even when the protected attribute labels are corrupted.

**Sensitivity to  $\lambda$ .** We measure the sensitivity of FaRM’s performance w.r.t  $\lambda$  (Equation 7) in the constrained setup. In Figure 7, we show the MDL of the target attribute  $y$  (in blue) and protected attribute  $g$  (in red) for DIAL and PAN16 (mention/gender) for different  $\lambda$  after 25 epochs of training. Ideally, we want MDL for protected attribute ( $g$ ) to be *large*, with a *small* target attribute ( $y$ ) MDL. We observe that when  $10^{-4} \leq \lambda \leq 1$ , the final performance of FaRM does not change much in terms of MDL. For  $\lambda = 10$ , we observe target attribute MDL is quite large, showcasing that the model is not able to converge on the target task. This is expected as the magnitude of the bias loss term  $[R^c(Z, \epsilon | \Pi^g) - R(Z, \epsilon)]$  (Equation 7) is much larger than  $CE(\hat{y}, y)$  term, and boosting it further with  $\lambda = 10$  makes it difficult for the target task loss to converge. Similarly, when  $\lambda \leq 10^{-5}$ , the bias term’s magnitude is much smaller compared to task loss, and a significant drop in  $g$ ’s MDL is observed for both datasets. However, we show that FaRM achieves similar performance over a broad spectrum of  $\lambda$  values, therefore reproducing the desired results does not require extensive hyperparameter tuning.

**Probing Word Embeddings.** A limitation of using FaRM for debiasing word embeddings is that distances in the original embedding space is not preserved. Mazur–Ulam theorem (Jamison, 2002) states that isometry for a mapping  $\phi : V \rightarrow W$  is preserved only if the function  $\phi$  is affine. As our feature map  $\phi(x)$  is non-linear, distances cannot be preserved using FaRM. Using a linear  $\phi(x)$  is

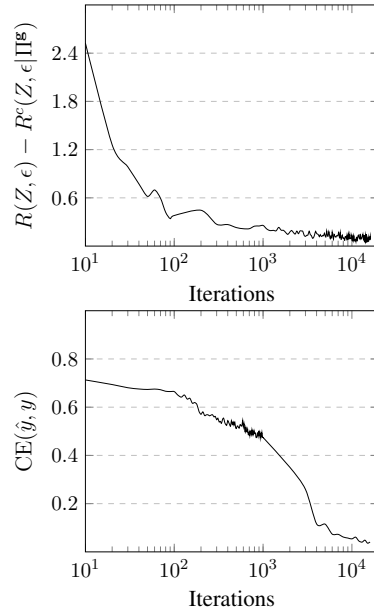


Figure 8: Loss evolution in a constrained setup with  $\lambda = 0.01$ . We observe that bias loss (top) starts converging earlier than the target loss (bottom).

also not ideal because it is not possible to guard a protected attribute against an attack by a non-linear probing network using an affine (linear) function. While a non-linear function does not preserve distances, we perform experiments to investigate if the debiased embeddings still possess relevant information for downstream tasks. In particular, we experiment with part-of-speech (POS) tagging and sentiment classification tasks described below:

(a) *Part-of-speech tagging:* We evaluate debiased embeddings obtained from FaRM for detecting POS tags in a sentence from Universal tagset (Petrov et al., 2012). GloVe embeddings achieve a F1-score of 95.2% on the POS tag prediction task. Embeddings from FaRM achieve a F1-score of 93.0%. This shows FaRM’s debiased embeddings still possess significant amount of morphological information about the language, which helps the tagger in POS prediction.

(b) *Sentiment Classification:* We also evaluate the embeddings for sentiment classification on the IMDb movies dataset (Maas et al., 2011). GloVe embeddings achieve an accuracy of 80.9% on this dataset, while FaRM achieves a performance of 74.6%. The drop in this task is slightly more compared to POS tagging, but FaRM is still able to achieve a decent performance on this task.

The experiment above showcase that even though distances in the original word embedding

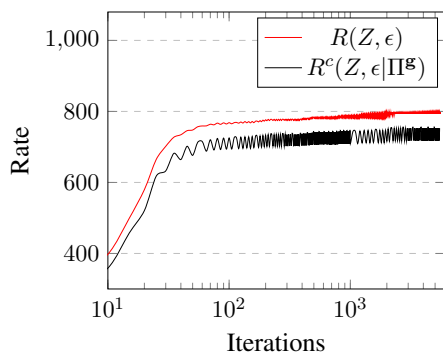


Figure 9: Loss evolution in an unconstrained setup. Both terms in the objective function:  $R(Z, \epsilon)$  (in **red**) and  $R^c(Z, \epsilon | \Pi^g)$  (in **black**) start increasing simultaneously.

space aren't preserved using FaRM, it still retains relevant information useful in downstream tasks.

**Evolution of loss components.** In the constrained setup, we evaluate how FaRM's loss components: target loss  $CE(\hat{y}, y)$  and bias loss  $[R(Z, \epsilon) - R^c(Z, \epsilon | \Pi^g)]$  evolve during training for DIAL dataset. In Figure 8, we observe that the bias term converges first followed by the target loss. This is expected as the magnitude of rate-distortion loss for bias is larger than target loss, which forces the model to minimize it first.

Next, we conduct a similar experiment for debiasing word embeddings in an unconstrained setup. In this case, we evaluate how FaRM's loss components  $R(Z, \epsilon)$  (in **red**) and  $R^c(Z, \epsilon | \Pi^g)$  (in **black**) evolve during training, shown in Figure 9. We observe that both loss terms in this setup start increasing simultaneously. The difference between these terms appear to remain constant in the later half of training.

**Limitations.** A limitation of FaRM is that we do not have a principled way for selecting a feature map function  $\phi(x)$ . In the unconstrained setup, we relied on empirical observations to decide the number of layers of the non-linear function. We observed that a 4-layer ReLU network sufficed for Biography classification and word embedding debiasing, but we had to employ a 7-layer network for controlled sentiment classification. For the constrained setup, BERT<sub>base</sub> proved to be expressive enough to perform debiasing in all setups. Future works can explore methods to quantify the rate gain  $\Delta J_u$  in each layer, and select network architectures based on that.

## 9 Conclusion

We proposed **Fairness-aware Rate Maximization** (FaRM), a novel debiasing technique based on the principle of rate-distortion maximization. FaRM is effective in removing protected information from representations in both unconstrained and constrained debiasing setups. Empirical evaluations show that FaRM outperforms prior works in debiasing representations by a large margin on several datasets. Extensive analysis showcase that FaRM is sample efficient, robust to label corruptions and minor hyperparameter changes. Future works can focus on leveraging FaRM for achieving fairness in complex tasks like language generation.

## References

- Jimmy Lei Ba, Jamie Ryan Kiros, and Geoffrey E Hinton. 2016. Layer normalization.
- Maria Barrett, Yova Kementchedjhieva, Yanai Elazar, Desmond Elliott, and Anders Søgaard. 2019. [Adversarial removal of demographic attributes revisited](#). In *Proceedings of the 2019 Conference on Empirical Methods in Natural Language Processing and the 9th International Joint Conference on Natural Language Processing (EMNLP-IJCNLP)*, pages 6330–6335, Hong Kong, China. Association for Computational Linguistics.
- Kanadpriya Basu, Treena Basu, Ron Buckmire, and Nishu Lal. 2019. Predictive models of student college commitment decisions using machine learning. *Data*, 4(2):65.
- Somnath Basu Roy Chowdhury, Sayan Ghosh, Yiyuan Li, Junier Oliva, Shashank Srivastava, and Snigdha Chaturvedi. 2021. [Adversarial scrubbing of demographic information for text classification](#). In *Proceedings of the 2021 Conference on Empirical Methods in Natural Language Processing*, pages 550–562, Online and Punta Cana, Dominican Republic. Association for Computational Linguistics.
- Su Lin Blodgett, Lisa Green, and Brendan O'Connor. 2016. [Demographic dialectal variation in social media: A case study of African-American English](#). In *Proceedings of the 2016 Conference on Empirical Methods in Natural Language Processing*, pages 1119–1130, Austin,

- Texas. Association for Computational Linguistics.
- Tolga Bolukbasi, Kai-Wei Chang, James Y. Zou, Venkatesh Saligrama, and Adam Tauman Kalai. 2016. [Man is to computer programmer as woman is to homemaker? debiasing word embeddings](#). In Advances in Neural Information Processing Systems 29: Annual Conference on Neural Information Processing Systems 2016, December 5-10, 2016, Barcelona, Spain, pages 4349–4357.
- John D. Burger, John Henderson, George Kim, and Guido Zarrella. 2011. [Discriminating gender on Twitter](#). In Proceedings of the 2011 Conference on Empirical Methods in Natural Language Processing, pages 1301–1309, Edinburgh, Scotland, UK. Association for Computational Linguistics.
- Maria De-Arteaga, Alexey Romanov, Hanna Wallach, Jennifer Chayes, Christian Borgs, Alexandra Chouldechova, Sahin Geyik, Krishnamurthy Kenthapadi, and Adam Tauman Kalai. 2019. Bias in bios: A case study of semantic representation bias in a high-stakes setting. In proceedings of the Conference on Fairness, Accountability, and Transparency, pages 120–128.
- Sunipa Dev, Tao Li, Jeff M Phillips, and Vivek Srikumar. 2020. [Oscar: Orthogonal subspace correction and rectification of biases in word embeddings](#). ArXiv preprint, abs/2007.00049.
- Jacob Devlin, Ming-Wei Chang, Kenton Lee, and Kristina Toutanova. 2019. [BERT: Pre-training of deep bidirectional transformers for language understanding](#). In Proceedings of the 2019 Conference of the North American Chapter of the Association for Computational Linguistics: Human Language Technologies, Volume 1 (Long and Short Papers), pages 4171–4186, Minneapolis, Minnesota. Association for Computational Linguistics.
- Yanai Elazar and Yoav Goldberg. 2018. [Adversarial removal of demographic attributes from text data](#). In Proceedings of the 2018 Conference on Empirical Methods in Natural Language Processing, pages 11–21, Brussels, Belgium. Association for Computational Linguistics.
- Yanai Elazar, Shauli Ravfogel, Alon Jacovi, and Yoav Goldberg. 2021. Amnesic probing: Behavioral explanation with amnesic counterfactuals. Transactions of the Association for Computational Linguistics, 9:160–175.
- Bjarke Felbo, Alan Mislove, Anders Søgaard, Iyad Rahwan, and Sune Lehmann. 2017. [Using millions of emoji occurrences to learn any-domain representations for detecting sentiment, emotion and sarcasm](#). In Proceedings of the 2017 Conference on Empirical Methods in Natural Language Processing, pages 1615–1625, Copenhagen, Denmark. Association for Computational Linguistics.
- Omar Ghailan, Hoda MO Mokhtar, and Osman Hegazy. 2016. Improving credit scorecard modeling through applying text analysis. institutions, 7(4).
- Ian J Goodfellow, Jean Pouget-Abadie, Mehdi Mirza, Bing Xu, David Warde-Farley, Sherjil Ozair, Aaron Courville, and Yoshua Bengio. 2014. [Generative adversarial networks](#). ArXiv preprint, abs/1406.2661.
- James E Jamison. 2002. [Isometries on Banach spaces: function spaces](#). Chapman and Hall/CRC.
- Armand Joulin, Edouard Grave, Piotr Bojanowski, and Tomas Mikolov. 2017. [Bag of tricks for efficient text classification](#). In Proceedings of the 15th Conference of the European Chapter of the Association for Computational Linguistics: Volume 2, Short Papers, pages 427–431, Valencia, Spain. Association for Computational Linguistics.
- Moshe Koppel, Shlomo Argamon, and Anat Rachel Shimoni. 2002. Automatically categorizing written texts by author gender. Literary and linguistic computing, 17(4):401–412.
- Yitong Li, Timothy Baldwin, and Trevor Cohn. 2018. [Towards robust and privacy-preserving text representations](#). In Proceedings of the 56th Annual Meeting of the Association for Computational Linguistics (Volume 2: Short Papers), pages 25–30, Melbourne, Australia. Association for Computational Linguistics.
- Ilya Loshchilov and Frank Hutter. 2019. [Decoupled weight decay regularization](#). In

- 7th International Conference on Learning Representations, ICLR 2019, New Orleans, LA, USA, May 6-9, 2019. [OpenReview.net](https://openreview.net).
- Yi Ma, Harm Derksen, Wei Hong, and John Wright. 2007. Segmentation of multivariate mixed data via lossy data coding and compression. IEEE transactions on pattern analysis and machine intelligence, 29(9):1546–1562.
- Andrew L. Maas, Raymond E. Daly, Peter T. Pham, Dan Huang, Andrew Y. Ng, and Christopher Potts. 2011. [Learning word vectors for sentiment analysis](#). In Proceedings of the 49th Annual Meeting of the Association for Computational Linguistics: Human Language Technologies, pages 142–150, Portland, Oregon, USA. Association for Computational Linguistics.
- Laurens Van der Maaten and Geoffrey Hinton. 2008. Visualizing data using t-sne. Journal of machine learning research, 9(11).
- Jan Macdonald, Stephan Waldchen, Sascha Hauch, and Gitta Kutyniok. 2019. [A rate-distortion framework for explaining neural network decisions](#). ArXiv preprint, abs/1905.11092.
- Ninareh Mehrabi, Fred Morstatter, Nripsuta Saxena, Kristina Lerman, and Aram Galstyan. 2019. [A survey on bias and fairness in machine learning](#). ArXiv preprint, abs/1908.09635.
- Dong Nguyen, Rilana Gravel, Dolf Trieschnigg, and Theo Meder. 2013. "how old do you think i am?" a study of language and age in twitter. In Proceedings of the International AAAI Conference on Web and Social Media, volume 7.
- Fabian Pedregosa, Gael Varoquaux, Alexandre Gramfort, Vincent Michel, Bertrand Thirion, Olivier Grisel, Mathieu Blondel, Peter Prettenhofer, Ron Weiss, Vincent Dubourg, et al. 2011. Scikit-learn: Machine learning in python. the Journal of machine Learning research, 12:2825–2830.
- Slav Petrov, Dipanjan Das, and Ryan McDonald. 2012. [A universal part-of-speech tagset](#). In Proceedings of the Eighth International Conference on Language Resources and Evaluation (LREC’12), pages 2089–2096, Istanbul, Turkey. European Language Resources Association (ELRA).
- Francisco Rangel, Paolo Rosso, Ben Verhoeven, Walter Daelemans, Martin Potthast, and Benno Stein. 2016. Overview of the 4th author profiling task at pan 2016: cross-genre evaluations. Working Notes Papers of the CLEF, 2016:750–784.
- Shauli Ravfogel, Yanai Elazar, Hila Gonen, Michael Twiton, and Yoav Goldberg. 2020. [Null it out: Guarding protected attributes by iterative nullspace projection](#). In Proceedings of the 58th Annual Meeting of the Association for Computational Linguistics, pages 7237–7256, Online. Association for Computational Linguistics.
- Alexey Romanov, Maria De-Arteaga, Hanna Wallach, Jennifer Chayes, Christian Borgs, Alexandra Chouldechova, Sahin Geyik, Krishnamurthy Kenthapadi, Anna Rumshisky, and Adam Kalai. 2019. [What’s in a name? Reducing bias in bios without access to protected attributes](#). In Proceedings of the 2019 Conference of the North American Chapter of the Association for Computational Linguistics: Human Language Technologies, Volume 1 (Long and Short Papers), pages 4187–4195, Minneapolis, Minnesota. Association for Computational Linguistics.
- Andrew Rosenberg and Julia Hirschberg. 2007. [V-measure: A conditional entropy-based external cluster evaluation measure](#). In Proceedings of the 2007 Joint Conference on Empirical Methods in Natural Language Processing and Computational Natural Language Learning (EMNLP-CoNLL), pages 410–420, Prague, Czech Republic. Association for Computational Linguistics.
- Shivashankar Subramanian, Xudong Han, Timothy Baldwin, Trevor Cohn, and Lea Frermann. 2021. [Evaluating debiasing techniques for intersectional biases](#). ArXiv preprint, abs/2109.10441.
- Ben Verhoeven and Walter Daelemans. 2014. [CLiPS stylometry investigation \(CSI\) corpus: A Dutch corpus for the detection of age, gender, personality, sentiment and deception in text](#). In Proceedings of the Ninth International Conference on Language

- Resources and Evaluation (LREC'14), pages 3081–3085, Reykjavik, Iceland. European Language Resources Association (ELRA).
- Ben Verhoeven, Walter Daelemans, and Barbara Plank. 2016. [Twisty: A multilingual Twitter stylometry corpus for gender and personality profiling](#). In [Proceedings of the Tenth International Conference on Language Resources and Evaluation \(LREC'16\)](#), pages 1632–1637, Portorož, Slovenia. European Language Resources Association (ELRA).
- Elena Voita and Ivan Titov. 2020. [Information-theoretic probing with minimum description length](#). In [Proceedings of the 2020 Conference on Empirical Methods in Natural Language Processing \(EMNLP\)](#), pages 183–196, Online. Association for Computational Linguistics.
- Edson RD Weren, Anderson U Kauer, Lucas Mizusaki, Viviane P Moreira, J Palazzo M de Oliveira, and Leandro K Wives. 2014. Examining multiple features for author profiling. [Journal of information and data management](#), 5(3):266–266.
- Qizhe Xie, Zihang Dai, Yulun Du, Eduard H. Hovy, and Graham Neubig. 2017. [Controllable invariance through adversarial feature learning](#). In [Advances in Neural Information Processing Systems 30: Annual Conference on Neural Information Processing Systems 2017, December 4-9, 2017, Long Beach, CA, USA](#), pages 585–596.
- Yaodong Yu, Kwan Ho Ryan Chan, Chong You, Chaobing Song, and Yi Ma. 2020. [Learning diverse and discriminative representations via the principle of maximal coding rate reduction](#). [ArXiv preprint](#), abs/2006.08558.
- Richard S. Zemel, Yu Wu, Kevin Swersky, Toniann Pitassi, and Cynthia Dwork. 2013. [Learning fair representations](#). In [Proceedings of the 30th International Conference on Machine Learning, ICML 2013, Atlanta, GA, USA, 16-21 June 2013, volume 28 of JMLR Workshop and Conference Proceedings](#), pages 325–333. JMLR.org.
- Brian Hu Zhang, Blake Lemoine, and Margaret Mitchell. 2018. Mitigating unwanted biases with adversarial learning. In [Proceedings of the 2018 AAAI/ACM Conference on AI, Ethics, and Society](#), pages 335–340.
- Han Zhao and Geoffrey J. Gordon. 2019. [Inherent tradeoffs in learning fair representations](#). In [Advances in Neural Information Processing Systems 32: Annual Conference on Neural Information Processing Systems 2019, NeurIPS 2019, December 8-14, 2019, Vancouver, BC, Canada](#), pages 15649–15659.
- Jieyu Zhao, Yichao Zhou, Zeyu Li, Wei Wang, and Kai-Wei Chang. 2018. [Learning gender-neutral word embeddings](#). In [Proceedings of the 2018 Conference on Empirical Methods in Natural Language Processing](#), pages 4847–4853, Brussels, Belgium. Association for Computational Linguistics.

## A Appendix

### A.1 Ablation: Unconstrained Debiasing

In this section, we present an ablation of FaRM where we utilize protected information loss of the unconstrained setup to mimic constrained debiasing. The modified objective function for unconstrained debiasing is shown as:

$$\mathcal{L}_U(Z, \Pi^g) = [R^c(Z, \epsilon | \Pi^g) - R(Z, \epsilon)] \quad (13)$$

We evaluate this objective function for word embedding debiasing task. We obtain gender prediction accuracy of 49.8% from the debiased embeddings, which slightly is better than the reported results in Table 1. However, rank of the debiased embedding matrix is 2 (original dimension: 300), which shows that most of the information (including gender) has been destroyed during debiasing. This shows the importance of maximizing the overall rate-distortion term  $R(Z, \epsilon)$ , which helps in retaining diverse information from the original embedding space.